Nanotechnology

PAPER

Highly selective etching of SiN_x over SiO_2 using ClF_3/Cl_2 remote plasma

To cite this article: Seong Jae Yoo *et al* 2023 *Nanotechnology* **34** 465302

View the article online for updates and enhancements.

You may also like

- MultipleEtchant Loading Effect and Silicon Etching in ClF_3 and Related Mixtures
Daniel L. Flamm, David N. K. Wang and Dan Maydan

- Effect of Conductive Additives and Surface Fluorination on the Electrochemical Properties of Lithium Titanate ($Li_{4/3}Ti_{5/3}O_4$)
Xiaohong Kang, Hidetoshi Utsunomiya, Takashi Achiha et al.

- Chemical Conditions of SiCNO Film Exposed to ClF_3 Gas
Kenta Hori, Hiroki Kawakami and Hitoshi Habuka

This content was downloaded from IP address 115.145.196.112 on 09/11/2023 at 06:49

YMTC
Exhibit 2020
Micron v. YMTC
IPR2025-00034

Ex. 2020-001

IOP Publishing Nanotechnology
Nanotechnology 34 (2023) 465302 (8pp) https://doi.org/10.1088/1361-6528/acec7a

Highly selective etching of SiN_x over SiO_2 using ClF_3/Cl_2 remote plasma

Seong Jae Yoo[1], Ji Eun Kang[1], You Jin Ji[1], Hyun Woo Tak[1], Byeong Ok Cho[2], Young Lae Kim[2], Ki Chan Lee[2], Jin Sung Chun[3], Yongil Kim[1], Dong Woo Kim[1] and Geun Young Yeom[1,4,*]

[1] School of Advanced Materials Science and Engineering, Sungkyunkwan University, 2066 Seobu-ro, Jangan-gu, Suwon-si, Gyeonggi-do 16419, Republic of Korea
[2] Research and Development Group, Wonik Materials Co. Ltd, Cheongju 28215, Republic of Korea
[3] Semiconductor R&D Center, Wonik IPS Co. Ltd, Pyeongtaek 17709, Republic of Korea
[4] SKKU Advanced Institute of Nano Technology (SAINT), Sungkyunkwan University, 2066 Seobu-ro, Jangan-gu, Suwon-si, Gyeonggi-do 16419, Republic of Korea

E-mail: dwkim111@gmail.com and gyyeom@skku.edu

Received 12 March 2023, revised 19 July 2023
Accepted for publication 2 August 2023
Published 29 August 2023

Abstract

Highly selective etching of silicon nitride over silicon oxide is one of the most important processes especially for the fabrication of vertical semiconductor devices including 3D NAND (Not And) devices. In this study, isotropic dry etching characteristics of SiN_x and SiO_2 using ClF_3/Cl_2 remote plasmas have been investigated. The increase of Cl_2 percent in ClF_3/Cl_2 gas mixture increased etch selectivity of SiN_x over SiO_2 while decreasing SiN_x etch rate. By addition of 15% Cl to ClF_3/Cl_2, the etch selectivity higher than 500 could be obtained with the SiN_x etch rate of ~8 nm min^{-1}, and the increase of Cl percent to 20% further increased the etch selectivity to higher than 1000. It was found that SiN_x can be etched through the reaction from Si–N to Si–F and Si–Cl (also from Si–Cl to Si–F) while SiO_2 can be etched only through the reaction from Si–O to Si–F, and which is also in extremely low reaction at room temperature. When SiN_x/SiO_2 layer stack was etched using ClF_3/Cl_2(15%), extremely selective removal of SiN_x layer in the SiN_x/SiO_2 layer stack could be obtained without noticeable etching of SiO_2 layer in the stack and without etch loading effect.

Supplementary material for this article is available online

Keywords: silicon nitride (SiN_x), silicon oxide (SiO_2), chlorine monofluoride (ClF_3), Cl_2, selective etching, remote plasma etching, 3D NAND

(Some figures may appear in colour only in the online journal)

1. Introduction

For the continuous improvement of semiconductor device performances, in addition to scaling down of device sizes, the devices with three dimensional (3D) structures such as fin-type field effect transistors (FinFETs) [1, 2] and gate-all around FETs [3, 4] are currently being developed. For these devices, because of miniaturization and complexity of structures, its fabrication requires various highly selective etch processes not only for anisotropic etching but also for isotropic etching. For example, for 3D Not-And (NAND) devices, which was developed to overcome the limitation of 2D structural integration, a bilayer stack (ON stack) composed of SiN_x and SiO_2 is formed, and extremely high selective removal of SiN_x layer over SiO_2 layer is necessary [5–7].

Currently, to selectively etch the SiN_x over SiO_2, a wet etching method using hot phosphoric acid(H_3PO_4) is generally used [8–10]. This method is very effective in etching the SiN_x layers selectively. But, as the number of ON stack is increased and the layer thickness is decreased, it is found that

* Author to whom any correspondence should be addressed.

 © 2023 IOP Publishing Ltd

Ex. 2020-002

it is difficult to etch the SiN_x uniformly due to the difficulty in solution penetration by surface tension and leaning of remaining thin SiO_2 layer [10, 11]. Also, it was found that some additives used to increase the etch selectivity of SiN_x over SiO_2 cause a problem of oxide regrowth [11, 12]. Therefore, a dry etching method that is isotropic and highly selective to SiO_2 is required for next generation high density 3D NAND flash memory fabrication [13]. Previous studies showed that highly selective dry etching of SiN_x over SiO_2 can be obtained with halogen gases such as CF_4 or NF_3 [13–16]. In these studies, very high etch selectivity higher than 100 has been obtained with gas mixtures (O_2, N_2, H_2) using plasma etching systems. However, even with encouraging results, for application to next generation 3D NAND device fabrication, many issues such as high global warming potentials (GWP) and contamination are encountered in using these gases [17–21]. Moreover, current semiconductor processes require much higher etch selectivity.

As previously shown, ClF_3/H_2 remote plasma was used for selective dry etching of SiN_x over SiO_2 mainly because GWP of ClF_3 is ~0 and contains a lot of halogen elements that are highly reactive to SiN_x and, at an optimized condition, SiN_x/SiO_2 etch selectivity over 200 could be achieved [22]. The reason for not using fluorocarbon of hydrofluorocarbon gases containing carbon in the etching was to increase the etch selectivity of SiN_x over SiO_2 by preventing the formation of CO through the reaction of O in SiO_2 with carbon. Here, in this study, Cl_2 was added to ClF_3 and the effect of Cl_2 addition on the etch characteristics SiN_x, SiO_2, and ON stack was investigated. The results showed that addition of small Cl_2 to ClF_3 increased the SiN_x etch selectivity to SiO_2 significantly and even higher than 1,000 even though the SiN_x etch rate was decreased with increasing the Cl_2 percentage. The etch mechanism was also suggested through plasma characterization and film surface analysis.

2. Method

Remote plasma-type inductively coupled plasma (ICP) etch system used in the experiment is shown in figure 1. A planar spiral-type ICP source was installed on the top of the chamber and quartz window was located below the ICP source to transmit ICP power to the plasma. To form a remote plasma source, dual anodized aluminum grids having holes out-of-aligned not to have ion to the substrate were located 20 cm below the ICP source. The size of the grid holes was 3 mm diameter and the distance between the grid was maintained at 1 cm. The process chamber was vacuumed using a dry pump without using a turbopump and the base pressure was kept lower than 40 mTorr. As the etching gases, ClF_3(>99.9%) and Cl_2(>99.999%) were used and these gases were fed to the process chamber. In addition, as a reference, ClF (>99.9%) was also used. 13.56 MHz RF power was applied to the ICP source through a L-type matching network while keeping the operating pressure at 200 mTorr with ClF_3/Cl_2 gas combinations. The substrate holder was cooled by a chiller or heated by a SiC heater.

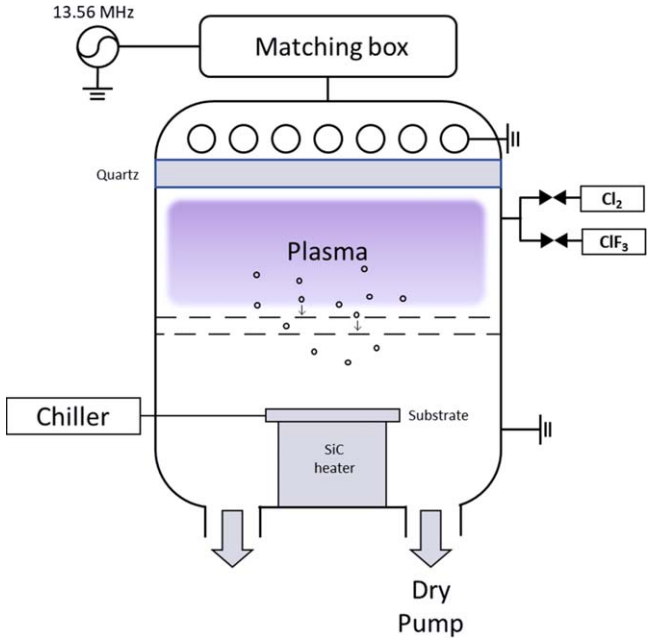

Figure 1. Schematic diagram of a remote type inductively coupled plasma (ICP) system used in the experiment. At the middle of the chamber, a dual grid was installed for prevention of ion bombardment and radical flow to the substrate.

SiN_x deposited by plasma enhanced chemical deposition and SiO_2 deposited by low pressure chemical vapor deposition fabricated by Wonik IPS Corp. for 3D NAND processing were used for experiment. The thickness of SiN_x and SiO_2 were 500 and 285 nm, respectively. In addition, 50-layer stack composed of SiO_2/SiN_x (ON) pairs was prepared to observe isotropic etching characteristics. In this ON pair stack, the thickness of each Si_3N_4 and SiO_2 layers was ~27 nm.

The etched amount of SiN_x and SiO_2 was measured by a spectroscopic ellipsometer (Nano-View SE MG-1000). To confirm isotropic etching in the 3D structure, the etch profiles of SiN_x/SiO_2 stacks were observed by field emission scanning emission microscopy (FE-SEM, Hitachi S-4700). The surface roughness of SiN_x and SiO_2 before and after the etching was measured using an atomic force microscope (AFM, Park System XE-100). The surface composition and chemical binding states of SiN_x and SiO_2 before and after the etching were observed using x-ray photoelectron spectroscopy (XPS, VG Microtech Inc., ESCA2000). The XPS data were evaluated after the peak shift based on C 1s (~285 eV) and the XPS narrow scan peaks were deconvoluted using an automated peak separation analysis software (PeakFit) after background was removed. To analyze the species in the ClF_3/Cl_2 plasma, an optical emission.

Spectrometer (OES, Isoplane SCT 3200; the blaze wavelength of 300 nm and grating of 1200 g min^{-1}) was installed on the plasma source chamber wall and the optical emission wavelength range from 200 to 1000 nm were measured. Byproduct gases during the etching exhausting to the vacuum system were observed with Fourier-transform

Ex. 2020-003

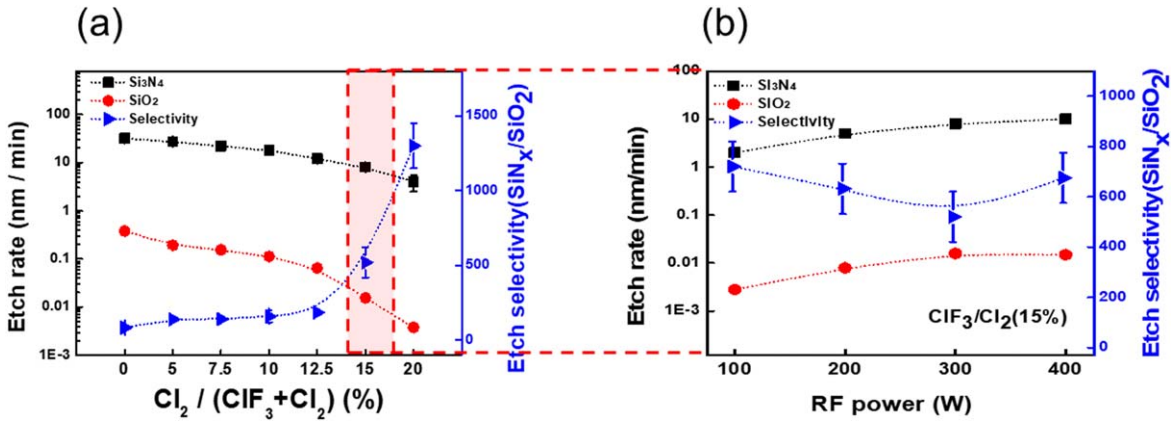

Figure 2. Etch characteristics of SiN_x and SiO_2 (a) as a function of Cl_2 percentage in ClF_3/Cl_2 remote plasma and (b) as a function of rf power for 15% of Cl_2 / (ClF_3+Cl_2) (%).

infrared spectroscopy (FT-IR, MIDAC 12000) installed after the dry pump.

3. Results and discussions

Using ClF_3/Cl_2 gas mixtures, the etch rates of SiN_x and SiO_2, and the etch selectivities of SiN_x/SiO_2 were investigated and the results are shown in figure 2(a). 200 sccm of ClF_3/Cl_2 total flow rate, 200 mTorr of operating pressure, 300 W of RF power, and 25 °C of substrate temperature were used while varying the ratio of $Cl_2/(ClF_3+Cl_2)$ from 0% to 20%. As shown in figure 2(a), when ClF_3 only used for the etching SiN_x, the etch rate of ~30 nm min^{-1} and the etch selectivity over SiO_2 of ~80 was obtained (the effect of operating pressure on etch rate of SiN_x and etch selectivity of SiN_x/SiO_2 for ClF_3 is also shown in supplementary information figure S1). With the increase of Cl_2 in the Cl_2/ClF_3 mixture, the SiN_x etch rate was decreased while increasing the etch selectivity, and, at ClF_3/Cl_2(20%), the etch rate was decreased to ~4 nm min^{-1} but the etch selectivity was increased to ⩾1000. And, when 15% Cl_2 was added to ClF_3 (ClF_3/Cl_2(15%)), the SiN_x etch rate was ~8 nm min^{-1} and the etch selectivity of SiN_x/SiO_2 was ⩾ 500. While keeping ClF_3/Cl_2(15%) and other process conditions, the RF power was varied from 100 to 400 Watts, the etch rates of SiN_x and etch selectivites of SiN_x/SiO_2 measured as a function of RF are shown in figure 2(b). As shown in figure 2(b), the increase of RF power increased etch rates of SiN_x from 2 to 10 nm min^{-1} but the etch selectivity was remained similar at ⩾500. It is believed that the increase of SiN_x etch rate without significantly varying the etch selectivity of SiN_x/SiO_2 with increasing the RF power is related to the increased radicals of Cl and F at similar ratios. Therefore, by varying other process variables in addition to the gas flow ratios of ClF_3/Cl_2, the improvement of etch characteristics would be possible (supplementary information figure S2). Also, when the RMS surface roughness values of SiN_x and SiO_2 measured by AFM before and after etching for 5 min were compared for etching with ClF_3 only and ClF_3/Cl_2(15%) using the etching conditions in figure 2(a), even though slight increase of surface roughness was observed for SiN_x etched with ClF_3 only, no noticeable change in surface roughness was observed for all SiO_2 surfaces and SiN_x etched with ClF_3/Cl_2(15%) (supplementary information figure S3).

To understand the etch behavior of SiN_x and SiO_2 observed as a function of ClF_3/Cl_2, dissociated species in the plasma were observed for various ClF_3/Cl_2 gas mixtures with 0~40% Cl_2 and the results are shown in figures 3(a) and (b) for wide wavelength (150–1000 nm) data of ClF_3plasma and ClF_3/Cl_2(15%) plasma, respectively. 10 sccm Ar was added in the gas mixtures for compensating electron density during OES peak intensity comparison without disturbing ClF_3/Cl_2 plasma characteristics. Other conditions are the same as those in figure 2(a). As shown in figures 3(a) and (b), the peaks related to F (685.5, 703.8 nm, etc) and the peaks related to Cl (837.6, 858.6 nm, etc) were observed in addition to added Ar peaks (750.4 nm, etc). In figure 3(c), the peaks related to F at 703.8 nm and Cl at 837.6 nm for Cl_2 percentage from 0% to 40% are shown after normalization with Ar peak intensity at 750.4 nm. As shown in figure 3(c), the Cl/Ar was increased and F/Ar was decreased with increasing Cl_2 percentage. Therefore, as shown in figure 3(d), the F/Cl was decreased almost linearly with increasing Cl_2 percentage from% 0 to 40%. Therefore, when the results in figure 2(a) are compared with OES data in figure 3(d), it can be seen that SiN_x etch rate and etch selectivity of SiN_x/SiO_2 are related to the relative ratios of F/Cl in the plasma. That is, higher F/Cl ratio in the plasma increases etch rates but decreases etch selectivity of SiN_x/SiO_2 and lower F/Cl ratio in the plasma decreases etch rates but increases etch selectivity of SiN_x/SiO_2.

Byproducts formed after the etching of SiN_x with ClF_3/Cl_2 remote plasmas were observed by FTIR installed after the dry pump and the results are shown in figure 4(a) before and after ClF_3/Cl_2(15%) remote plasma generation and (b) with different Cl_2 ratios in ClF_3/Cl_2 during SiN_x etching. The other process conditions are the same as those in figure 2(a). As shown in figure 4(a), after the plasma generation, the decrease of ClF_3 peak intensity was observed while showing the increase of SiF_4 peak intensity related to etching of SiN_x with F, however, no $SiCl_4$ peak intensity related to etching of SiN_x with Cl could be observed (Also, no

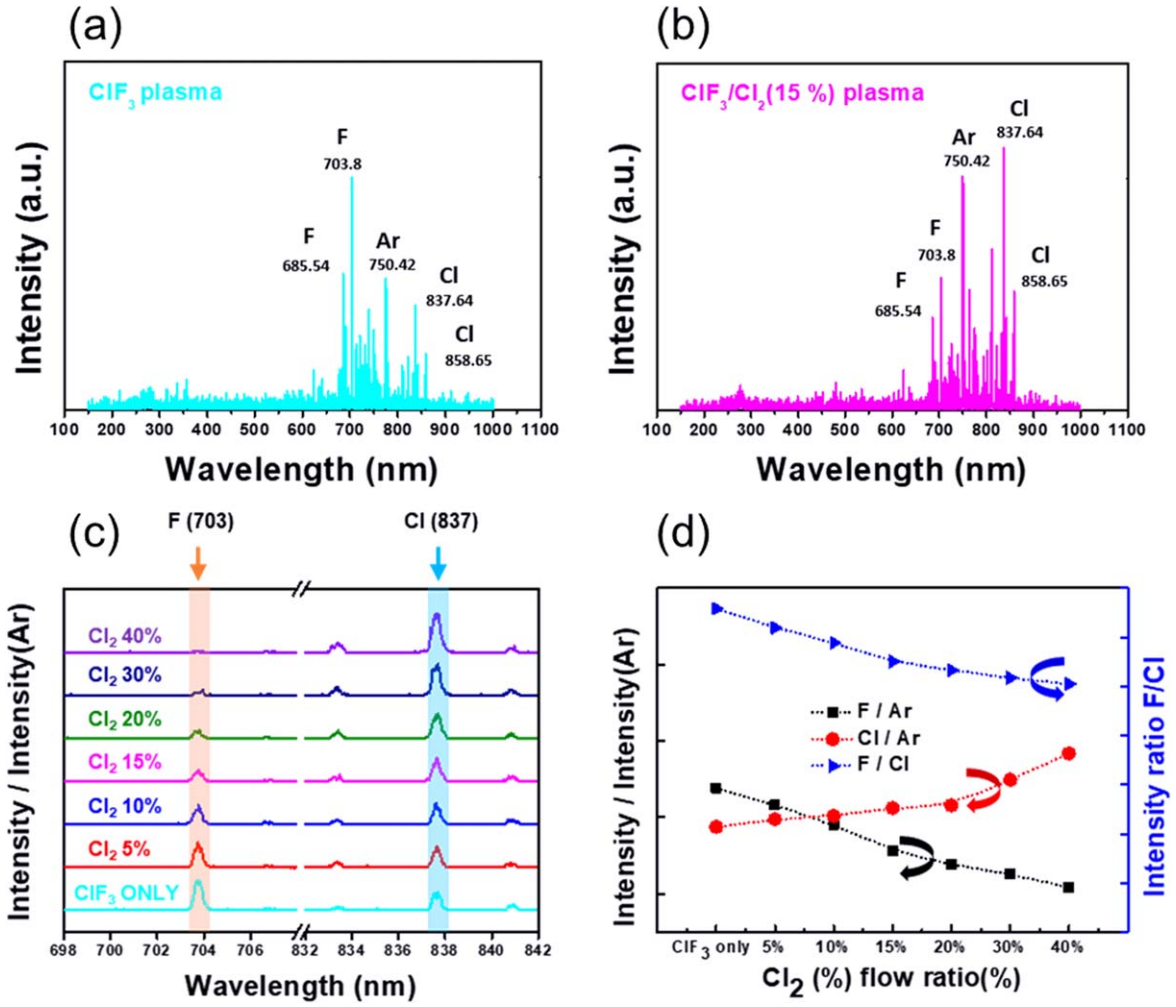

Figure 3. OES data of plasma generated with (a) ClF_3 and (b) ClF_3/Cl_2(15%) plasma. (c) OES data for plasma generated with ClF_3/(0%–40% Cl_2) showing narrow wavelength range from 100 to 1000 nm showing F peak and Cl peak normalized by Ar peak at 750.4 nm. (d) optical emission intensities of F (703 nm) / Cl (837 nm) and F (703 nm), Cl (837 nm) normalized by the intensity of Ar (750.4 nm).

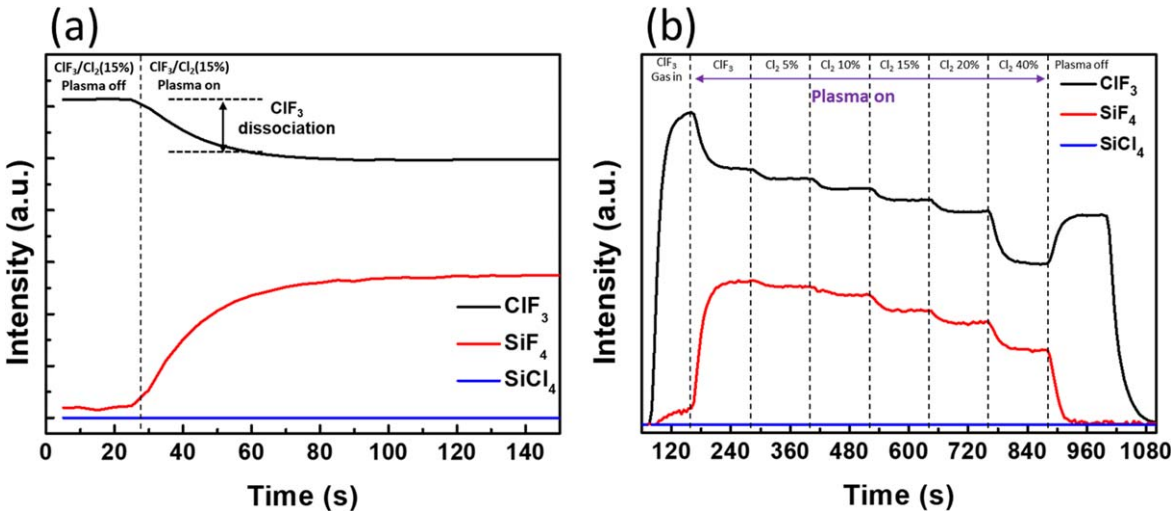

Figure 4. FTIR data of (a) before and after ClF_3/Cl_2(15%) plasma generation during SiN_x etching and (b) byproducts during SiN_x etching with ClF_3/Cl_2 plasma with different Cl_2 ratios from 0% to 40%.

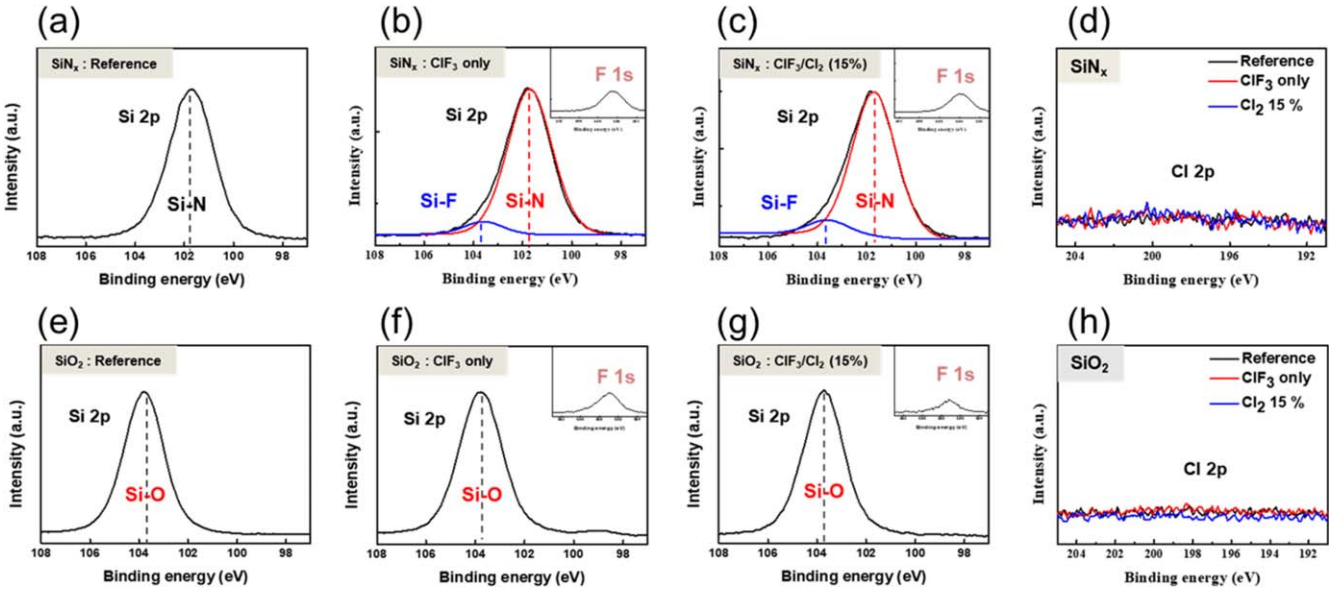

Figure 5. XPS narrow scan data of Si 2p, F 1s, and Cl 2p measured on the surfaces of blank SiN_x and SiO_2 after etching for 5 min using ClF_3/Cl_2 remote plasma. (a)–(d) are for SiN_x and (e)–(h) are for SiO_2. (a) and (d) are Si references, (b) and (f) are Si 2p and F 1s after etching with ClF_3 only, (c) and (g) are Si 2p and F 1s after etching with ClF_3/Cl_2(15%), and (d) and (h) are Cl_2 2p for reference and after etching with ClF_3 only and ClF_3/Cl_2(15%).

peak intensities related to Cl_2 and N_2 could not be observed because FTIR cannot measure diatomic molecules or noble gases such as H_2, Cl_2, He, Ar, etc which do not have absorbance bands in the infrared region of the spectrum). As shown in figure 4(b), when the Cl_2 percent was increased every 2 min from 0% to 40%, the intensity related to ClF_3 was decreased every 2 min due to the lower percentage of ClF_3 in ClF_3/Cl_2 gas mixture and the peak intensity related to SiF_4 was also decreased similarly with the decrease of ClF_3 peak intensity without showing any peak intensity related to $SiCl_4$ even with the increase of Cl_2 to 40%. Therefore, as observed in OES results in figure 3, the main etchant involved in the etching of SiN_x was F not Cl.

Using XPS, the surface binding states of SiN_x and SiO_2 before and after etching using ClF_3 and ClF_3/Cl_2(15%) were investigated, and the results are shown in figures 5(a)–(d) for SiN_x and (e)–(h) for SiO_2 (wide scan data can be found in supplementary information figure S4). Figures 5 (a) and (e) are Si 2p references, (b) and (f) are Si 2p and F 1s after etching with ClF_3 only, (c) and (g) are Si 2p and F 1s after etching with ClF_3/Cl_2(15%), and (d) and (h) are Cl 2p for reference and after etching with ClF_3 only and ClF_3/Cl_2(15%). The other etch conditions are the same as those in figure 2(a). As shown in figures 5(a) and (e), Si 2p peaks of the references were located at 101.7 eV for SiN_x and 103.4 eV for SiO_2 which are related to Si–N bond and Si–O bond, respectively. As shown in figures 5(b) and (c), after etching using ClF_3 and ClF_3/Cl_2(15%), a peak at 103.6 eV related to Si–F bond in addition to Si–N bond peak was observed in Si 2p of SiN_x (F 1s peak at 687 eV was also observed as shown in inset figure). However, in case of SiO_2, as shown in figures 5(f) and (g), after etching using ClF_3 and ClF_3/Cl_2(15%), no peak related to Si–F bond in addition to Si–O bond peak was observed in Si 2p of SiO_2 even though F 1s peak was also observed at 687 eV (inset figure). Therefore, it can be found that, on SiN_x surface, F atoms are easily chemisorbed, however, on SiO_2 surface, F atoms are adsorbed but not easily chemisorbed. Therefore, F radicals generated by ClF_3/Cl_2 plasmas react more with SiN_x than SiO_2. Also, as shown in figures 5(d) and (h), even with high Cl percentage of ClF_3/Cl_2(15%), no peak related to Cl (198.5 eV) was observed for both surfaces of SiN_x and SiO_2 indicating no adsorption of Cl even with high Cl radicals in ClF_3/Cl_2 plasmas.

From the above results, it can be deduced that, during the etching of SiN_x using ClF_3/Cl_2 plasmas, Si–N bond (−355 KJ mol^{-1}) can be replaced to Si–Cl bond (−381 KJ mol^{-1}) and more easily to Si–F bond (−565 KJ mol^{-1}), however, due to the higher binding energy of Si–F compared to Si–Cl, the Si–Cl bonds appear to be replaced to Si–F bonds and these Si–F bonds (both from Si–N to Si–F and from Si–N to Si–F through Si–Cl) lead to etching of SiN_x by forming SiF_4. However, in the case of SiO_2, Si–O bond (−452 KJ mol^{-1}) could be replaced to Si–F bond but cannot be replaced to Si–Cl bond (−381 KJ mol^{-1}) due to the lower binding energy of Si–O bond compared to that of Si–Cl bond (the relationship of bond energies for SiN_x and SiO_2 with Cl and F are shown in supplementary figure S5). Also, because no Si–F bonds are found on etched SiO_2 surface, it is found to be also difficult for Si–O bonds to be easily replaced to Si–F bonds possibly due to high energy barrier for reaction from Si–O to Si–F. That is, with decreasing F/Cl ratio in the plasma, SiN_x can be etched through the reaction from Si–N to Si–Cl and Si–F but SiO_2 has difficulty in etching due to the no reaction from Si–O to Si–Cl and extremely low reaction from Si–O to Si–F. Therefore, as shown in figure 2(a), higher etch selectivity of SiN_x/SiO_2 appears to be obtained with the decrease of F/Cl ratio in the plasma. Also, when the ratio of F/Cl is decreased

Ex. 2020-006

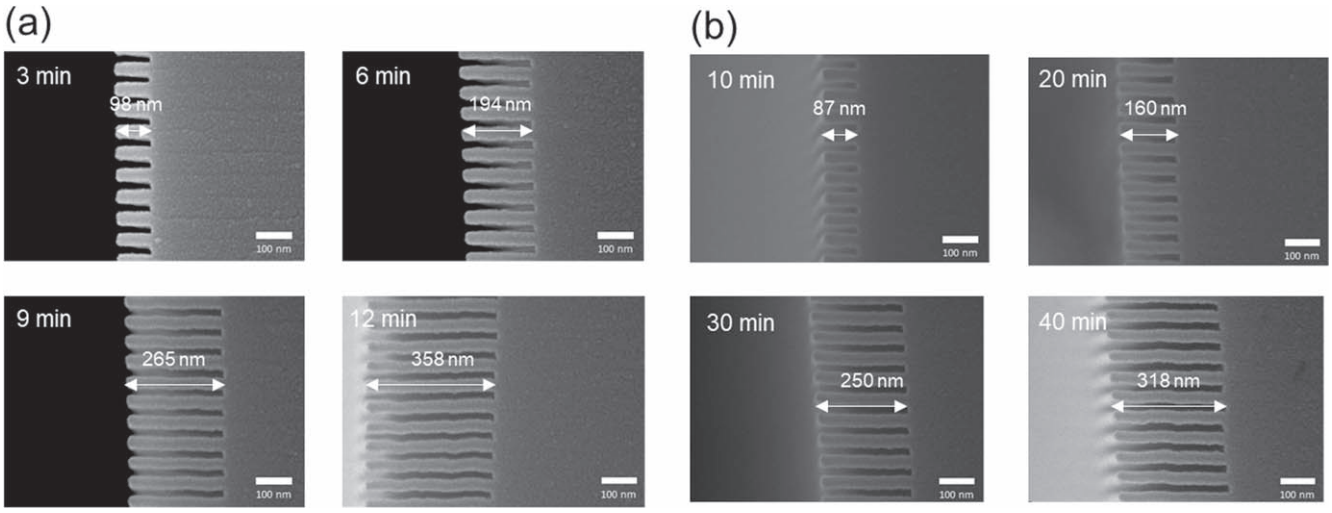

Figure 6. Cross-sectional SEM images of ON stacks as a function of etch time. Etched with (A) ClF_3 plasma and (b) ClF_3/Cl_2(15%) plasma.

in the gas mixture of ClF_3/Cl_2, both etch rates of SiO_2 and SiN_x are decreased due to lower reactivity of both materials with Cl but the etch selectivity of SiN_x/SiO_2 is increased due to higher etch rate of SiN_x compared to SiO_2 at the same F/Cl ratio.

Using ClF_3 and ClF_3/Cl_2(15%), actual ON stack composed of SiO_2 (27 nm thick)/SiN_x (27 nm thick) layers was etched and figure 6 shows cross-section SEM images of ON stack etched with (a) ClF_3 and (b) ClF_3/Cl_2(15%) as a function of etching time. The etch conditions are the same as those in figure 2(a). As shown in figures 6(a) and (b), with increase of etch time, due to the high etch selectivity of SiN_x/SiO_2, only the etching of SiN_x layer was observed and the etch depth was increased with time as shown in figures 6(a) and (b). From figures 6(a) and (b), the SiN_x etch depth with etch time was measured and the results are shown in figures 7(a) for ClF_3 and (b) for ClF_3/Cl_2(15%). As shown in figure 7, the etch depth was increased almost linearly with increase of etch time without having loading effect until ~400 nm deep SiN_x was etched by showing ~30 nm min^{-1} for ClF_3 and ~8 nm min^{-1} for ClF_3/Cl_2(15)%.

The remaining oxide layer thickness in the ON stack after etching of 380–400 nm deep SiN_x was observed, and the SEM images of remaining oxide layers are shown in figure 8(a) for ClF_3 and (b) for ClF_3/Cl_2(15%). The other etch conditions are the same as those in figure 2(a). To see the remaining SiO_2 thickness more clearly, SEM images containing the top SiO_2 layer in the ON stack were included. As shown in figure 8(a), for ClF_3, due to the low selectivity of SiN_x/SiO_2 of ~80 as shown in figure 2(a), the remaining SiO_2 layer showed thin front thickness of ~21 nm due to long etch time and thick back thickness of ~27 nm due to short etch time. Also, the thickness of top SiO_2 layer showed ~21 nm due to long exposure to remote plasma. However, for ClF_3/Cl_2(15%), due to the higher etch selectivity of $\geqslant$ 500, no noticeable differences in remaining SiO_2 layer thickness among front, back, and top SiO_2 layers could be observed by

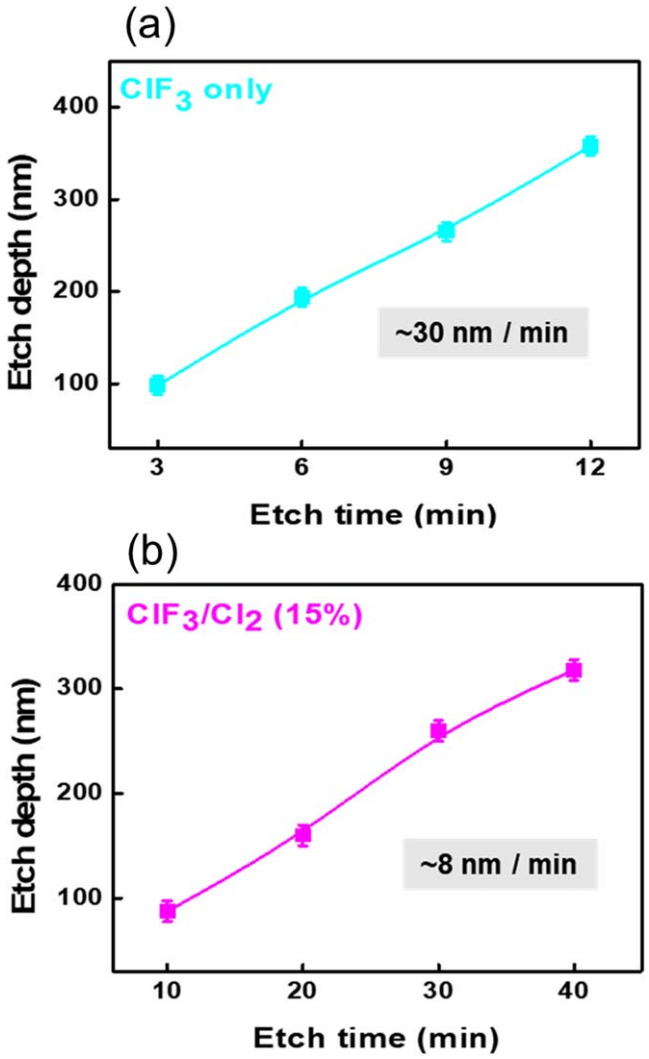

Figure 7. Etch depth of SiN_x in SiO_2/SiN_x stack measured as a function of etch time with (a) ClF_3 only and (b) ClF_3/Cl_2 (15%) plasmas.

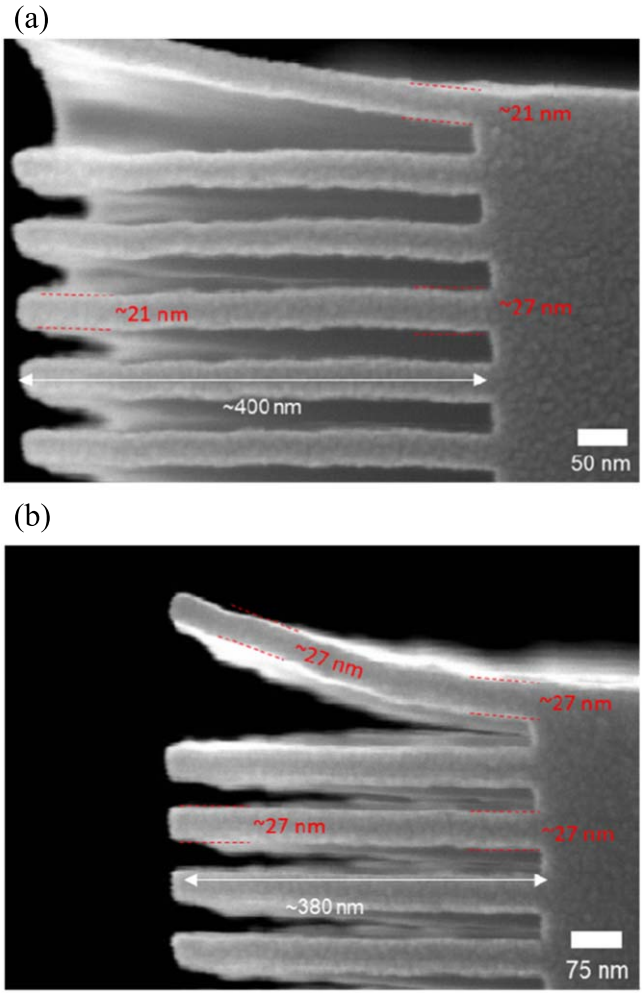

Figure 8. Cross-sectional SEM images of remaining oxide layers in SiN_x/SiO_2 stack after etching of 380 ~400 nm deep SiN_x with (a) ClF_3 plasma and (b) ClF_3/Cl_2(15%) remote plasma.

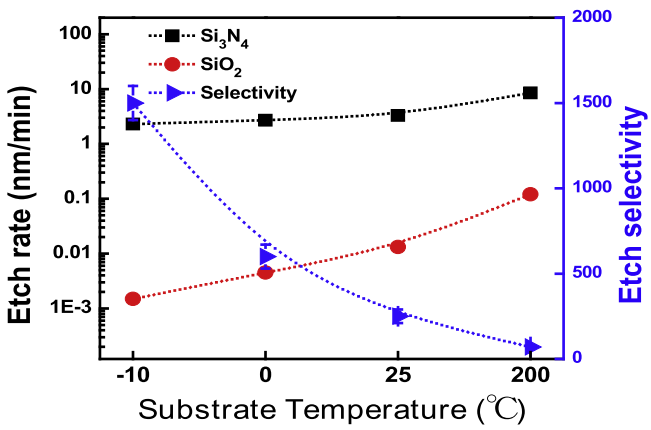

Figure 9. Etch characteristics of SiN_x and SiO_2 as a function of temperature for ClF remote plasma at 300 W of rf power.

showing ~27 nm. Therefore, it is believed that, by using ClF_3/Cl_2 gas mixtures, SiN_x layers in ON layer stack composed of SiN_x and SiO_2 can be etched extremely selectively.

Finally, to verify the importance of F/Cl ratio in the selective etching of SiN_x over SiO_2 using Cl/F base gases, ClF was used instead of ClF_3, and figure 9 shows the etch characteristics of SiN_x and SiO_2 using ClF observed as a function of substrate temperature. As the process conditions, 200 sccm of ClF flow rate, 200 mTorr of operating pressure, and 300 W of RF power were used. At room temperature, the SiN_x etch rate was ~3 nm min^{-1} and the etch selectivity of SiN_x/SiO_2 was 250 compared to ~8 nm min^{-1} of SiN_x etch rate and ~80 of SiN_x/SiO_2 etch selectivity for ClF_3. Therefore, it is believed that the etch rate and etch selectivity for ClF_3/Cl_2 and ClF are basically dependent on the Cl/F ratio in the gas mixture (the effects of RF power and operating pressure on SiN_x etch rate for ClF are shown in supplementary figure S6 and cross-sectional SEM images are shown in figure S7). The decrease of substrate temperature decreased the SiN_x etch rate but increased etch selectivity of SiN_x/SiO_2, and, at −10 °C, the etch selectivity close to 1500 could be obtained with the SiN_x etch rate of ~2.3 nm min^{-1}.

4. Conclusion

In this study, selective isotropic dry etching of SiN_x over SiO_2 on the ON stack for 3D semiconductor devices was studied using ClF_3/Cl_2 remote plasmas. The results showed that the increase of Cl_2 percentage in ClF_3/Cl_2 plasmas decreased etch rates of both SiN_x and SiO_2, but the etch selectivity of SiN_x/SiO_2 was increased and, with the ClF_3/Cl_2(15%) plasma, the etch rate of 8 nm min^{-1} and etch selectivity of $\geqslant$ 500 could be achieved. In the Cl/F based plasmas, it was suggested that SiN_x can be etched both by F and Cl by replacing Si–N bond in SiN_x to Si–F and Si–Cl bonds and also by replacing Si–Cl to Si–F. On the contrary, SiO_2 can be etched only by replacing Si–O bond in SiO_2 to Si–F bond, however, the reaction from Si–O bond to Si–F bond appears to be very low at room temperature. Therefore, the decreased F/Cl ratio in the plasma with the increase of Cl_2 in the ClF_3/Cl_2 plasmas increased etch selectivity of SiN_x/SiO_2. Using ClF_3/Cl_2(15%) plasma at room temperature, SiN_x layers in SiO_2/SiN_x layer stack could be etched extremely selectively without noticeable loss of SiO_2 layer thickness. It is believed that highly selective and isotropic dry etching of SiN_x/SiO_2 stack required for next generation various 3D device fabrication can be achieved with Cl/F based gases by controlling the Cl/F ratios.

Acknowledgments

This work was supported by the Technology Innovation Program (or Industrial Strategic Technology Development Program-Materials Parts Technology Development-Package Type) (20022471, Development of Equipment and Process for Cleaning the Surface and Removing By-products of HAR Contact with Self-Diagnosis Function) funded By the Ministry of Trade, Industry & Energy (MOTIE, Korea).

Data availability statement

All data that support the findings of this study are included within the article (and any supplementary files).

ORCID iDs

Seong Jae Yoo https://orcid.org/0000-0003-3700-6476
Geun Young Yeom https://orcid.org/0000-0002-1176-7448

References

[1] Auth C *et al* 2012 *Proc. Symp. VLSI Technology* p 131
[2] Natarajan S *et al* 2014 *IEDM Tech. Dig.* **71** 3.7.1–.3
[3] Waldron N, Merckling C, Teugels L, Ong P, Ibrahim S A U, Sebaai F, Paurghaderi A, Barla K, Collaert N and Thean A V Y 2014 *IEEE Electron Device Lett.* **35** 1097
[4] Song Y, Zhang C, Dowdy R, Chabak K, Mohseni P K, Choi W and Li X 2014 *IEEE Electron Device Lett.* **35** 324
[5] Seo D, Bae J S, Oh E, Kim S and Lim S 2014 *Microelectron. Eng.* **118** 66–71
[6] Tanaka H *et al* 2007 *IEEE Symp. VLSI Technol.* 14–5
[7] Jung S *et al* 2006 *Int. Electron Devices Meeting (San Francisco, CA, USA)* pp 1–4
[8] van Gelder W and Hauser V E 1967 *J. Electrochem. Soc.* **114** 869
[9] Sundaram K B, Sah R E, Baumann H, Balachandran K and Todi R M 2003 *Microelectron. Eng.* **70** 109
[10] Bassett D, Printz W and Furukawa T 2015 *ECS Trans.* **69** 159
[11] Kim T, Son C, Park T and Lim S 2020 *Microelectron. Eng.* **221** 111191
[12] Bassett D W and Rotondaro A L P 2016 *Solid State Phenom.* **255** 285
[13] Kastenmeier B E E, Matsuo P J and Oehrlein G S 1999 *J. Vac. Sci. Technol.* A **17** 3179–84
[14] Kastenmeier B E E, Matsuo P J, Oehrlein G S and Langan J G 1998 *J. Vac. Sci. Technol.* A **16** 2047–56
[15] Volynets V *et al* 2020 *J. Vac. Sci. Technol.* A **38** 023007
[16] Jung J E *et al* 2020 *J. Vac. Sci. Technol.* A **38** 023008
[17] Raju R, Kudo D, Kubo Y, Inaba T and Shindo H 2003 *Jpn. J. Appl. Phys.* **42** 280
[18] Ying W and Leory L 1998 *J. Vac. Sci. Technol.* A **16** 1582
[19] Lee S, Oh J, Lee K and Sohn H 2010 *J. Vac. Sci. Technol.* B **28** 131
[20] Lee H K and Yu J S 2009 *J. Korean Phys. Soc.* **54** 1816–23
[21] Park J W, Chae M G, Kim D S, Lee W O, Song H D, Choi C and Yeom G Y 2018 *J. Phys. D: Appl. Phys.* **51** 445201
[22] Lee W O *et al* 2022 *Sci Rep.* **12** 5703

Ex. 2020-009